

Medial temporal lobe atrophy patterns in early- versus late-onset amnestic Alzheimer's disease

Anika Wuestefeld^{1#}, Alexa Pichet Binette¹, Danielle van Westen^{2,3}, Olof Strandberg¹, Erik Stomrud^{1,4}, Niklas Mattsson-Carlsgren^{1,5,6}, Shorena Janelidze¹, Ruben Smith^{1,4}, Sebastian Palmqvist^{1,4}, Hannah Baumeister⁷, David Berron^{1,7}, Paul A. Yushkevich⁸, Oskar Hansson^{1,4}, Nicola Spotorno^{1*}, Laura EM Wisse^{2##}

Author affiliations

1 Clinical Memory Research Unit, Department of Clinical Sciences Malmö, Lund University, 22242 Lund, Sweden

2 Department of Diagnostic Radiology, Clinical Sciences, Lund University, 22242 Lund, Sweden

3 Image and Function, Skåne University Hospital, 22242 Lund Sweden

4 Memory Clinic, Skåne University Hospital, 20502 Malmö, Sweden

5 Department of Neurology, Skåne University Hospital, 22242 Lund, Sweden

6 Wallenberg Center for Molecular Medicine, Lund University, 22184 Lund, Sweden

7 German Center for Neurodegenerative Diseases (DZNE), 39120 Magdeburg, Germany

8 Penn Image Computing and Science Laboratory (PICSL), Department of Radiology, University of Pennsylvania, Philadelphia 19104, USA

* The authors contributed equally to this work.

Correspondence to:

Laura Wisse, PhD

Department of Diagnostic Radiology, Lund University

Klinikgatan 13B

SE-222 42, Lund, Sweden

E-mail: lemwisse@gmail.com

Anika Wuestefeld, MSc

Clinical Memory Research Unit

Department of Clinical Sciences Malmö, Lund University

Klinikgatan 28, Room C1103b

SE-222 42 Lund, Sweden

E-mail: anika.wuestefeld@gmail.com

Abstract

Background: The medial temporal lobe (MTL) is hypothesized to be relatively spared in early-onset Alzheimer's disease (EOAD). Yet, detailed examination of MTL subfield volumes and drivers of atrophy in amnestic EOAD is lacking.

Methods: BioFINDER-2 participants with memory impairment, abnormal amyloid- β status and tau-PET were included. Forty-one EOAD individuals aged ≤ 65 years and, as comparison, late-onset AD (LOAD, ≥ 70 years, $n=154$) and A β -negative cognitively unimpaired controls were included. MTL subregions and biomarkers of (co-)pathologies were measured.

Results: AD groups showed smaller MTL subregions compared to controls. Atrophy patterns were similar across AD groups, although LOAD showed thinner entorhinal cortices compared to EOAD. EOAD showed lower WMH compared to LOAD. No differences in MTL tau-PET or transactive response DNA binding protein 43-proxy positivity was found.

Conclusions: We found *in vivo* evidence for MTL atrophy in amnestic EOAD and overall similar levels to LOAD of MTL tau pathology and co-pathologies.

Keywords: tau-PET imaging, amyloid-beta, MRI, medial temporal lobe subregions, aging, *in vivo*, amnestic AD, early-onset, late-onset, amygdala segmentation protocol, TPD-43

Background

Early-onset Alzheimer's disease (EOAD) is commonly defined by a clinical onset before the age of 65 years and is one of the most common types of early-onset neurodegenerative dementia (1). It shares the presence of main neuropathological features, i.e., fibrillar amyloid- β (A β) and hyperphosphorylated tau, with late-onset LOAD (age >65), but clinical features and other characteristics tend to differ between EOAD and LOAD (1). For example, there is evidence for less semantic memory impairment and a more aggressive course with more neurofibrillary tangle (NFT) pathology in EOAD compared to LOAD (1,2).

While prior research has investigated clinical, genetic or pathological differences in EOAD vs. LOAD, for example (3–6), many studies define EOAD only by age of onset. Thus, various clinical phenotypes, such as amnestic or non-amnestic EOAD, posterior cortical atrophy (PCA), or primary progressive aphasia (PPA) (7), have been grouped together as EOAD group as they are more common in younger age than for late-onset AD (1). Due to this grouping, observed differences between EOAD vs. LOAD may not be applicable to all clinical phenotypes. For example, the medial temporal lobe (MTL) has previously been found to be relatively spared in EOAD compared to LOAD in several studies (8–10). However, it is unclear if this applies to amnestic EOAD given the common grouping of clinical phenotypes. Moreover, fine-grained changes in MTL subfield atrophy patterns have not been investigated. MTL subfields are heavily involved in memory function (11) but subserve different functions (12,13). Additionally, the cytoarchitectonic and functionally different MTL subfields are differently affected in AD and other neurodegenerative diseases (14–16). The involvement of the MTL in amnestic EOAD is not well characterized, therefore it is of importance to investigate whether the MTL is affected in EOAD and to what extent the atrophy pattern differs from the more common amnestic LOAD (17).

In addition to A β and NFT, co-pathologies are also common in AD (18) and can affect the clinical course of the disease as well as atrophy patterns in the brain (18–20). Common AD co-pathologies, such as cerebrovascular disease (CVD) or transactive response DNA binding protein 43 (TDP-43) pathology often occur in the MTL (21,22). Therefore, MTL atrophy patterns in amnestic AD are likely partially influenced by the presence of such co-pathologies. It has been suggested that co-pathologies are common in EOAD, albeit less than in LOAD, and contribute substantially to cognitive impairment in EOAD (5). However, it is unclear if this equally applies to all the phenotypes of EOAD including amnestic EOAD.

In this cross-sectional study we aim to investigate if MTL atrophy occurs in individuals with amnestic early-onset cognitive impairment (EOAD). To this end, we aim to compare MTL subfield differences across amnestic EOAD with the LOAD group and with cognitively normal controls as reference. Secondary aims include (I) investigating similar comparisons for neocortical composite regions in order to establish whether potential differences between EOAD and LOAD groups are specific to the MTL, and (II) assessing if common co-pathologies are present in EOAD vs. LOAD, and in comparison to healthy controls. Lastly, we explore if MTL atrophy is associated with AD pathologies and co-pathologies in the amnestic EOAD group. Exploratory analyses focus on (I) cognitive performance in amnestic EOAD and (II) comparisons with non-amnestic EOAD and LOAD groups.

Methods

Participants

We included 534 cognitively impaired from a memory clinic setting and unimpaired participants from population-based studies in the city of Malmö (23) older than 50 years from the Swedish BioFINDER-2 study (NCT03174938) who underwent magnetic resonance

imaging (MRI) and tau-PET. The study was approved by the ethical review board in Lund, Sweden, and all study participants provided written informed consent.

Inclusion criteria for the EOAD group were (I) mild cognitive impairment (MCI, MMSE \geq 24) or AD (MMSE \geq 20; see details in (23)), (II) 50-65 years of age, and who (III) were A β and tau positive accordingly to cerebrospinal fluid (CSF) A β 42/A β 40 ratio and tau-PET respectively, and (V) performed 1.5 standard deviations below age- and education-based norms on the Alzheimer's Disease Assessment Scale-Cognitive subscale (ADAS-cog) delayed word list recall (24). Additionally, patients between 65-70 years of age, who indicated their age of onset was before 65 on the Cognitive Impairment Questionnaire (CIMP-QUEST) and fulfilled all the other criteria were included as EOAD. The LOAD group included only patients with age \geq 70 years while the other criteria were shared between EOAD and LOAD. The gap of five years between EOAD and LOAD was chosen to minimize the possibility that EOAD cases were included in the LOAD group. Additionally, in secondary analyses, we included non-amnestic EOAD (naEOAD) and LOAD (naLOAD) participants that had the same group definitions as EOAD and LOAD except that the non-amnestic groups performed within age- and education-based norms on the episodic memory test. We focused only on cases who were A β - and tau-positive to ensure that the observed memory or cognitive impairments were at least partly due to AD proteinopathies.

Two control groups were included, one for EOAD and one for LOAD, given the inherent age differences between the patient groups. The control groups were (I) cognitively unimpaired, (II) A β negative, (III) performed within age- and education-based norms on the ADAS-cog delayed word list recall, and (IV) were selected with the same age range as respective EOAD or LOAD group.

Cerebrospinal fluid biomarkers

For a majority of the participants (n=514), CSF levels of A β 42 and A β 40 were measured with the Roche Elecsys platform (Roche Diagnostics International Ltd., Basel, Switzerland) as described previously by Hansson et al. (25). For the remaining participants (n=11), Lumipulse G (Fujirebio, n=9) or Meso-Scale Discovery (MSD; n=2) assays, were used to quantify concentration of A β 42 and A β 40. All CSF handling followed a standardized protocol (26,27). To determine A β -positivity a cut-off for CSF A β 42/A β 40 ratio was used with previously described thresholds obtained using Gaussian Mixture Modeling (Elecsys: 0.080; Lumipulse G: 0.072; MSD: <0.077) (28–30).

Cognitive assessment

Participants' cognitive functioning was estimated with the Mini-Mental State Examination (MMSE) (31), the Alzheimer's Disease Assessment Scale-Cognitive Subscale (ADAS-Cog) delayed word list recall (24), animal fluency (32), Boston Naming Test-15 (BNT-15) (33), Trail-Making Test B (34), Symbol digit modalities test (35), and the visual object and space perception (VOSP) battery subtest cubes (36). The scores were z-transformed using A β -cognitively unimpaired individuals under the age of 40 from BioFINDER-2 (n=99; MMSE \geq 26). These cognitive measures were chosen in order to capture various aspects of human cognition, such as memory, visuospatial functioning, language, and processing speed.

Imaging protocol

MRI

T1-weighted, T2-weighted, and Fluid attenuated inversion recovery (T2-weighted FLAIR) images were acquired on a Siemens MAGENTOM Prisma 3T scanner (Siemens Healthineers, Erlangen, Germany) with a 64-channel head coil. Whole brain T1-weighted images (Magnetization Prepared – Rapid Gradient Echo, MPRAGE) were acquired with the following parameters: in-plane resolution=1 \times 1 mm 2 , slice thickness=1 mm, repetition time

(TR)=1900 ms, echo time (TE)=2.54 ms, flip-angle=9. Coronal T2-weighted images were acquired using a turbo spin echo sequence (in-plane resolution=.4x.4 mm², slice thickness=2 mm, TR=8240 ms, TE=52 ms, flip-angle=150°) with hippocampal orientation. Similarly, axial T2-weighted FLAIR images were acquired (TR = 5000 ms, TE = 393 ms, TA = 4:37 min with the same resolution and field of view of the T1-weighted images).

Structural MRI processing and analysis

Using the Automated Segmentation of Hippocampal Subfields (ASHS) packages for T1- and T2-weighted MR images (37–40), MTL subregions were automatically segmented. To obtain hippocampal subfield volumes (Subiculum, cornu ammonis (CA) 1, dentate gyrus (DG)) the T2-weighted package was used (40). Anterior and posterior hippocampus (HC), and MTL cortical thickness measures (entorhinal cortex (ERC), Brodmann area (BA) 35 (≈transentorhinal cortex), BA36, and parahippocampal cortex) were extracted using the T1-weighted MRI package. Whole amygdala volumes were extracted using ASHS from a new atlas for T1-weighted MRI updated with an amygdala label created following a newly developed protocol (see supplementary methods, sFig. 1-10, sTable 1-2). Volumes of hippocampal subregions and the amygdala were corrected for ICV using volume-to-ICV fractions.

De Flores and colleagues (41) suggested that the ratio between anterior HC and parahippocampal cortex (measured with T1-ASHS) as a promising marker to assess the presence of TDP-43 pathology in dementia cases with AD neuropathologic change and was previously validated against post-mortem data. They propose a cut-off of 693.44 for this marker, indicating the presence of TDP-43 pathology for individuals with a ratio below this cut-off. Following their approach, a ratio between anterior HC volume and parahippocampal cortical thickness was calculated after regressing out ICV for anterior HC and age for both measures and the above-mentioned cut-off was applied.

After applying FreeSurfer 6 (<https://surfer.nmr.mgh.harvard.edu/>) to the T1-weighted image to obtain mean cortical thickness estimates, the neocortex was parcellated into five composite regions based on the Desikan-Killiany atlas. Average cortical thickness was extracted from the five composite regions consisting of: the lateral temporal (superior, middle, and inferior temporal, banks of the superior temporal sulcus, transverse temporal, temporal pole), lateral parietal (postcentral, inferior and superior parietal, supramarginal), medial parietal (paracentral, isthmus, posterior cingulate, precuneus), frontal (superior frontal, rostral and caudal middle frontal, pars opercularis, pars triangularis, pars orbitalis, lateral and medial orbitofrontal, precentral, paracentral, frontal pole), and occipital (cuneus, lateral occipital, lingual, pericalcarine) cortices.

As supplementary analyses, the Longitudinal Early-onset Alzheimer's Disease Study (LEADS) signature mean thickness, comprising primarily temporal and parietal regions, was calculated, see (42), and compared between groups.

All regions of interest were averaged across hemispheres. All regions of interest were z-scored to facilitate comparisons between the measures using A β - cognitively unimpaired individuals under the age of 40 from BioFINDER-2 (n=99; MMSE \geq 26) as reference group.

[¹⁸F]RO948 tau-PET

Tau-PET scans were acquired with a digital GE Discovery MI Scanner (General Electric Medical Systems). Tau-PET was performed 70-90 minutes post-injection of \sim 370 MBq of [¹⁸F]RO948. Details of the PET reconstruction have been published previously (43). The Swedish Medical Products Agency and the local Radiation Safety Committee at Skåne University Hospital, Sweden approved the PET imaging.

Tau-PET processing and analysis

Standardized uptake value ratios (SUVR) were calculated using an inferior cerebellar reference region for [¹⁸F]RO948-PET (tau-PET) (44). Using the geometric transfer matrix

method (45), partial volume correction (PVC) was performed. See Leuzy et al. (43) for a detailed description of our processing pipeline.

[¹⁸F]RO948-PET positivity was defined using a previously defined cut-off of a SUVR>1.362 (43) based on Gaussian Mixture Modeling in the temporal meta-ROI corresponding to Braak I-IV (46).

Tau-PET uptake was measured in two early regions (I) a composite MTL region from ASHS comprising ERC and BA35 from ASHS and (II) the amygdala from ASHS. The decision to use only ERC and BA35 was based on two aspects: (I) it reduces the potential bias caused by off target binding that typically occur around the hippocampus, (II) ERC and BA35 typically show the earliest accumulation of cortical tau pathology (14). Using clusters previously defined with an event-based modelling (EBM) approach, see (47), tau-PET composite measures were calculated for four EBM-based regions of interest (lateral temporal, parietal, frontal, occipital/motor), that match the neocortical composite regions. Lastly, a composite tau-PET SUVR was calculated for the LEADS signature (42).

White matter hyperintensity volume processing and analysis

Using FreeSurfer 7.2 Sequence Adaptive Multimodal SEGmentation (SAMSEG) functionality (48,49), white matter hyperintensities (WMH) were segmented from the T2-weighted FLAIR sequence. Whole brain WMH volumes were calculated per participant, corrected for ICV (using volume-to-ICV fractions) and log-transformed. This measure was used for primary analyses. Due to the distribution of the data (many participants with very low values), WMH volumes were also split into low/high based on median-split and used in sensitivity analyses.

Statistical analyses

Analyses were performed in R 4.0.2 (50). All p-values were controlled for the false discovery rate (FDR, Benjamini–Hochberg procedure). P-values were considered statistically

significant at $p < 0.05$. Group comparisons did not by default include age as a covariate, since the AD groups are defined by age. Only comparisons between controls and respective AD groups included age as covariate in sensitivity analyses.

Differences in demographic variables were tested using t-tests or chi-square tests. We examined group differences between EOAD and LOAD with respective controls and with each other for demographics and cognitive measures.

For our main aim, we examined group differences between EOAD and LOAD with respective controls and with each other for volume/thickness of the MTL regions of interest (3 comparisons) using one-way ANCOVAs along with post-hoc Tukey's HSD Test for multiple comparisons, including sex as covariate. We also investigate the interaction between age group (young vs. old) and diagnosis (CU vs. AD) in a linear regression model for each region in order to investigate if morphological metrics (i.e. volume or thickness) are differently affected by aging and disease state.

In addition, we characterized the EOAD and LOAD groups further by examining group differences between EOAD and LOAD with respective controls and with each other. This analysis was conducted, first, for the thickness of neocortical composite regions. We used ANCOVA to investigate group differences and performed linear regression models for each region with the interaction between age and diagnosis. Second, groups were compared for all biomarkers of AD- and co-pathologies. We used ANCOVA for continuous outcomes and logistic regression for categorical variables to assess group differences for the positivity on the aHC/PHC ratio (MRI-based proxy for potential TDP-43 positivity), as well as binarized WMH volume (low vs. high). In all analyses, sex was included as covariate.

As sensitivity analyses, age was included as covariate for comparisons between AD groups and controls. Second, for comparisons of AD- and co-pathologies, we included also CSF A β 42/A β 40 ratio as a covariate to investigate if differences between all group

comparisons were influenced by A β . Additional analyses additionally investigated group differences between EOAD and LOAD for the both LEADS signature thickness and tau-PET SUVR.

Secondary analyses

As exploratory analyses, we aim to investigate if different pathologies could explain lower region of interest volume/thickness within the EOAD group. To this end, we performed linear regressions predicting region of interest volume/thickness using biomarkers of AD- and co-pathologies including age and sex as covariates.

We explored group comparisons for cognitive performance (ADAS-cog delayed word recall, animal fluency, trail-making test B, VOSP cube, BNT-15). ANOVAs were used including sex and education as covariates. We also explore if differences in volume/thickness were associated with cognitive performance within the EOAD group, including education level, age, and sex as covariates.

In a final step, we also explored group comparisons for the amnestic and non-amnestic EOAD and LOAD groups.

Results

Demographics

The whole sample consisted of 534 older adults (56.9% female, mean age 69.2, mean education 12.8 years, 47.4% were *APOE- ϵ 4* carriers). The demographics of the EOAD (n=41) and LOAD (n=154) groups as well as the two control groups are shown in Table 1. Comparing EOAD vs. LOAD, no differences in sex, education, or *APOE* status were observed. A significant difference between LOAD and respective controls was observed for sex (lower proportion of males in the AD groups), and, as expected, *APOE* status (higher proportion of *APOE- ϵ 4* carriership in the AD groups). There was no difference in diagnosis between EOAD

and LOAD groups. Despite selecting AD patients and controls from the same age range, age was significantly, but marginally, different between AD groups and the respective controls, likely due to non-normal distributions within the AD groups. While the age difference is likely negligible, we did adjust for age in sensitivity analyses when comparing the AD groups to their respective control groups.

Table 1. Characteristics of the sample.

	YCU	OCU	EOAD	LOAD	Total	p-value YCU- EOAD	p-value OCU- LOAD	p-value EOAD- LOAD
N	188	151	41	154	534	-	-	-
Diagnosis						-	-	.713
CU	188 (100)	151 (100)	0 (0)	0 (0)	339 (63.5)			
MCI	0 (0)	0 (0)	16 (39.0)	65 (42.2)	81 (15.2)			
AD	0 (0)	0 (0)	25 (61.0)	89 (57.8)	114 (21.3)			
Sex (female)	103 (54.8)	99 (65.5)	20 (48.8)	82 (53.2)	304 (56.9)	.485	.029	.611
Age	58.6±4.89	77.3±3.38	61.0±4.82	76.2±3.92	69.2±9.76	.005	.008	-
Range	51.0 – 69.0	70.3 – 85.0	50.9 – 69.4 ^a	70.1 – 85.1	50.9 – 85.1			
Education (years)	13.2±3.12	12.4±3.74	14.1±3.33	12.5±4.79	12.8±3.86	.116	.816	.052
Missing	2 (1.1)	0 (0.0)	1 (2.4)	6 (3.9)	9 (1.7)			
APOE-ε4 allele +	85 (45.2)	29 (19.2)	25 (61.0)	114 (74.0)	253 (47.4)	.066	<.001	.116
CSF Aβ42/40 +^b	0 (0.0)	0 (0.0)	41 (100)	154 (100)	195 (36.5)	-	-	-

Continuous variables are displayed as mean±SD. Categorical variables are displayed as n (%). ^a individuals who reported an age-of-onset under 65 were included in the EOAD group. ^b Aβ positivity: <.08 on CSF Aβ42/40 ratio.

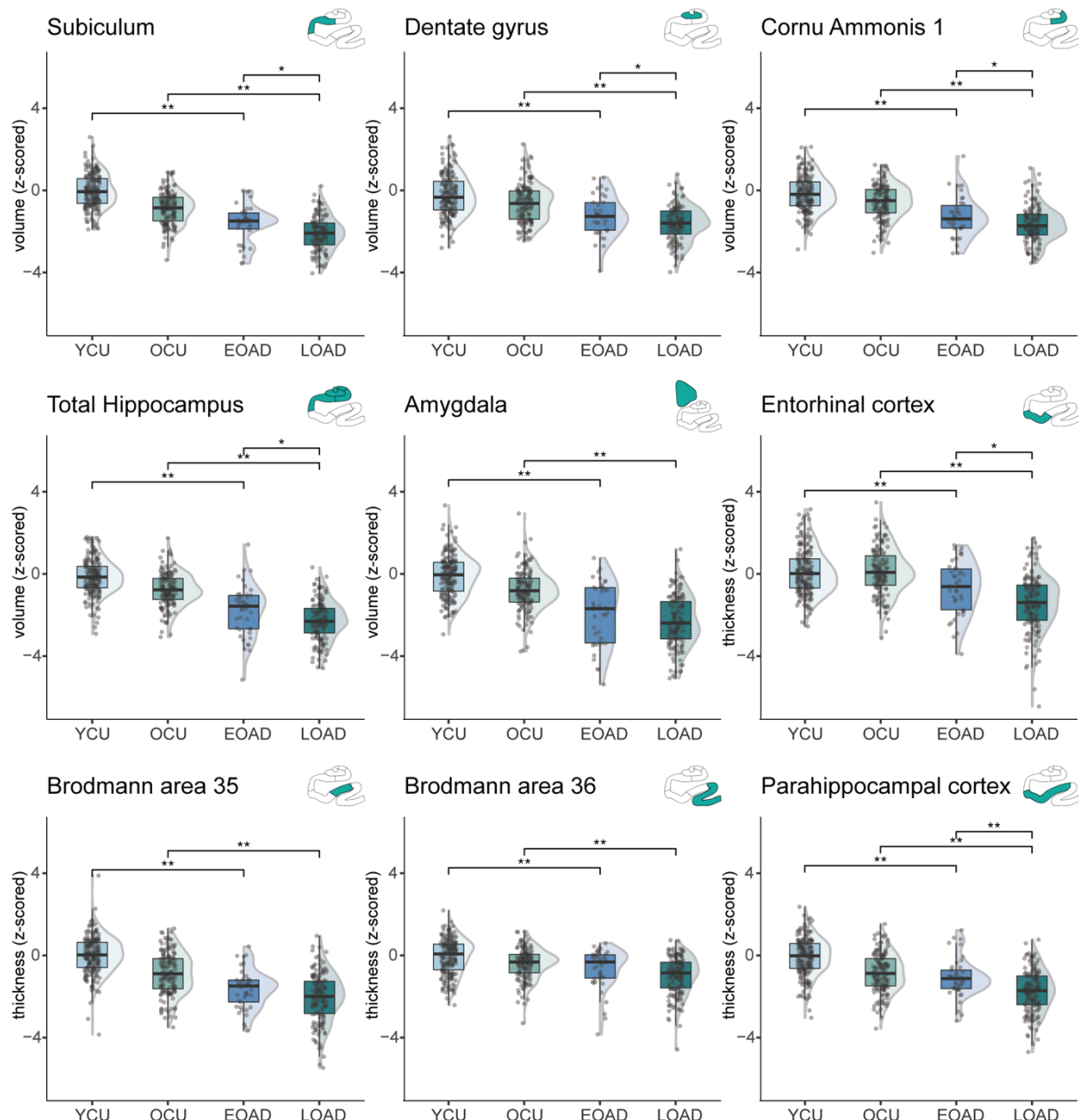
Abbreviations: Aβ=amyloid-beta; AD=Alzheimer's disease; CU=cognitively unimpaired; CSF=cerebrospinal fluid; EOAD=early-onset cognitive impairment, LOAD=late-onset cognitive impairment; MCI=mild cognitive impairment; OCU=older cognitively unimpaired controls; SD=standard deviation; YCU=younger cognitively unimpaired controls.

Amnestic EOAD shows medial temporal lobe subfield involvement

A statistically significant difference in mean value was found for all MTL regions of interest for both EOAD and LOAD compared to respective control groups (Fig. 1, supplementary results sTable 3). The biggest differences comparing EOAD with controls were observed in amygdala, BA35, and total hippocampus (z-score mean differences = 1.89, 1.70, -1.68 respectively, all p<.001). The biggest differences comparing LOAD with controls were observed in entorhinal cortex, amygdala, and total hippocampus (mean differences = 1.59, 1.55, 1.55 respectively, all p<.001). These results indicate similar atrophy patterns across the

medial temporal lobe (sFig. 11) between EOAD and LOAD, which was also confirmed by the lack of statistically significant interactions between age and diagnosis (sTable 4). The only exception was ERC where larger atrophy in LOAD appears and the interaction between age group and diagnosis was significant (sTable 4). These results contrast with previous reports which suggested limited involvement of the MTL in EOAD (see sTable 3). Including age as covariate did not change these results (see sTable 3).

Figure 1. EOAD and LOAD group differences in medial temporal lobe subfield volume/thickness.



ANOVAs were performed for each comparison. Significant differences are shown for FDR-corrected p-values. The ROI measures were z-scored based on young cognitively unimpaired individuals (<40, CSF A β 42/40 -). Results for the neocortical regions are included in the supplementary information. Abbreviations: EOAD=early-onset Alzheimer's Disease; LOAD=late-onset Alzheimer's disease; OCU=older controls; YCU=younger controls.

Focusing on the differences between EOAD and LOAD, significantly lower volume or thickness was found in LOAD compared to EOAD in five regions: subiculum (mean difference=0.50, $p_{FDR}=0.004$), dentate gyrus (mean difference=0.38, $p_{FDR}=0.042$), Cornu Ammonis 1 (mean difference=0.50, $p_{FDR}=0.042$), entorhinal (mean difference=0.78, $p_{FDR}=0.003$), and parahippocampal cortex (mean difference=0.68, $p_{FDR}<0.001$). Also, total hippocampal volume differed between EOAD and LOAD (mean difference=0.50, $p_{FDR}=0.011$, Fig. 1, sTable 3).

Further characterization of amnestic EOAD and LOAD

Neocortical thickness differences in amnestic EOAD vs. LOAD for frontal and lateral temporal cortices

As additional analyses, potential differences in thickness of neocortical regions in EOAD and LOAD were investigated. When comparing AD groups with their respective controls, a statistically significant difference was found for all neocortical regions of interest (sFig. 12A). The pattern of atrophy between EOAD and LOAD compared with respective controls was similar for all regions except for lateral and medial parietal cortices, for which the interaction between age group and diagnosis was also significant, indicating more prominent atrophy in the EOAD group (sFig. 12B). Additionally, significantly lower lateral temporal and frontal thickness was found in LO- compared to EOAD ($p_{FDR}=0.031$, 95%-C.I.=[-0.728, -0.051] and $p_{FDR}=0.014$, 95%-C.I.=[-0.841, -0.116] respectively; sFig. 12).

Lastly, comparisons of thickness in the LEADS signature were performed. Both EOAD and LOAD showed significantly thinner thickness compared to controls but no differences between EOAD and LOAD were observed (see sFig. 13).

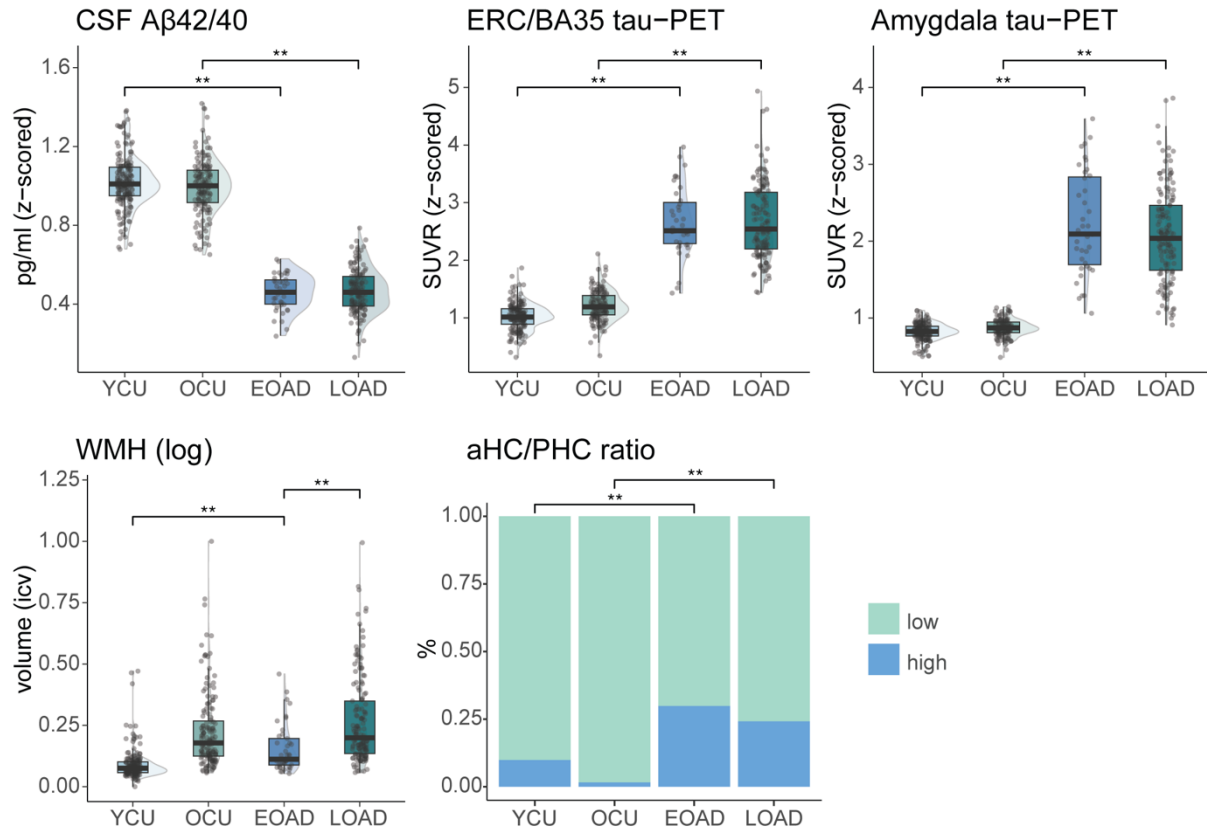
Amnestic EOAD shows a similar AD- and co-pathology burden as amnestic LOAD compared to controls

In a next step, we investigated potential differences in amnestic EOAD vs. LOAD with regards to common pathologies often accumulating in and related to MTL atrophy. Comparing AD groups with respective controls, a statistically significant difference in mean value was found for most AD pathologies and co-pathologies, indicating significantly higher pathology burden in the AD groups (MTL tau-PET SUVR, aHC/PHC ratio as TDP-43 proxy, CSF A β 42/A β 40 ratio; Fig. 2, supplementary material sTable 5). Only the total volume of WMH did not differ significantly between LOAD and controls ($p_{FDR}=.085$). The results remained consistent when including age as covariate, except that a significant difference between LOAD and controls was found for WMH ($p_{FDR}=.033$, see supplementary results sTable 6).

Focusing on the differences between EOAD and LOAD, we found a statistically significant higher mean value for WMH in LOAD compared to EOAD ($p_{FDR}<0.001$, 95%-C.I.=[0.056, 0.170]; Fig. 2; see supplementary sTable 5 and sFig. 14 for results using a dichotomized white matter hyperintensity measure). No differences in biomarkers of AD (MTL tau-PET and CSF A β 42/A β 40 ratio) were observed between EOAD and LOAD (Fig. 2). Additionally, no differences between EOAD and LOAD were observed in the proportion of positivity for MRI-based proxy of TDP-43 pathology (Fig. 2, sTable 5). Results of these group comparisons did not change when accounting for CSF A β 42/A β 40 ratio in the models.

Comparisons of tau-PET uptake in all four neocortical composite regions and the LEADS signature show higher uptake in AD groups compared to controls and EOAD showed a significantly higher tau-PET uptake in these neocortical composite regions compared to LOAD (see sTable 5, sFig. 13 and sFig. 15).

Figure 2. EOAD and LOAD group differences in AD pathologies and co-pathologies.



Separate ANOVAs were performed for each comparison. Significant differences are shown for FDR-corrected p-values. aHC/PHC ratio is an approximation of TDP-43 pathology. Abbreviations: aHC=anterior hippocampus; CSF=cerebrospinal fluid; EBM=event-based modelling; EOAD=early-onset Alzheimer's Disease; LOAD=late-onset Alzheimer's disease; PET=positron emission tomography; PHC=parahippocampal cortex; SAA=seeding amplification assay; SUVR=standardized uptake value ratio; OCU=older controls; WMH=white matter hyperintensities; YCU=younger controls.

Association between AD- and co-pathologies and atrophy in amnestic EOAD

In order to explore potential associations between AD- and co-pathologies and the structural measures, we focused only on the regions of interest which showed significant differences between EOAD and LOAD (total hippocampus (including subiculum, dentate gyrus, and cornu ammonis 1), entorhinal, parahippocampal; see sFig. 16).

Only the proxy of the presence of TDP-43 pathology was significantly associated with smaller total hippocampal volumes (std. $\beta = -.63$, $p_{FDR} < 0.001$). However, this association may be due to the definition of the measure considering the anterior hippocampus constitutes a large proportion of total hippocampal volume.

Cognitive performance in amnestic EOAD

Exploring group differences in cognitive performance, worse performance of the AD groups compared to respective controls was observed for all cognitive measures, while lower verbal fluency and naming abilities in LOAD compared to EOAD were observed (see sTable 7). No significant associations between MTL atrophy and performance on cognitive domains dependent on the MTL (episodic memory, naming, semantic fluency) were found for the amnestic EOAD group (see sFig. 17).

Comparison between amnestic and non-amnestic EOAD and LOAD

Demographic information on the non-amnestic AD (naEOAD: n=7; naLOAD: n=16) are provided in the supplementary material (sTable 8). Both amnestic AD groups showed lower MTL, but not neocortical, volume/thickness compared to non-amnestic AD (see sTable 9, sFig. 18-19). Subiculum volume and BA35 thickness were significantly smaller in amnestic vs. non-amnestic EOAD (see sTable 9, sFig. 18). The amnestic, compared to the non-amnestic AD groups showed higher amygdala tau-PET uptake. Non-amnestic LOAD showed larger WMH volumes compared to amnestic LOAD (see sTable 10, sFig. 20).

Discussion

The major aim of this cross-sectional study was to investigate if the MTL is affected in amnestic EOAD by comparing this group to amnestic LOAD atrophy patterns and respective controls in fine-grained MTL subregions from a highly characterized cohort and using a new reliable automated whole amygdala segmentation. In contrast with previous reports (8–10), amnestic EOAD, as well as LOAD, showed significantly smaller volumes of MTL regions compared to controls. LOAD, compared to EOAD, was found to have smaller volumes/thickness in the MTL only for hippocampus, entorhinal, parahippocampal cortex, and in the neocortical regions in lateral temporal and frontal cortex. To further characterize the AD

groups, we focused on biomarkers of AD and non-AD pathologies that often affect the MTL.

The EOAD grouped showed higher neocortical tau-PET uptake but lower WMH burden, compared to LOAD. However, no differences were observed for our proxy of TDP-43. Lastly, the proxy of TDP-43 positivity was associated with smaller hippocampal volumes indicating a potential involvement in driving atrophy in this region.

Our results show that the MTL is affected in amnestic AD, irrespective of age. This may seem in contrast with previous reports showing evidence of relative sparing of the MTL in EOAD (1,51,52). However, since prior studies commonly grouped all EOAD subtypes together with, for example, with PCA, PPA, or non-amnestic EOAD, except e.g. (53), it is possible that MTL atrophy in these studies was concealed by other phenotypes. The importance of the MTL in memory function (13), suggests that an amnestic type of AD should be associated with MTL atrophy, regardless of age of onset, a notion that is supported by our findings.

Even though we observed lower MTL thickness in amnestic EOAD when comparing with controls, LOAD still shows more atrophy within the MTL (e.g., lower thickness in entorhinal compared to EOAD). This may be due to several reasons. First, there may be non-specific aging effects on these cortical structures leading to more atrophy in the older patient group. Second, for some individuals, pathologies may have a longer duration of accumulation in these regions, potentially exerting an effect on structure for a longer duration resulting in more atrophy. Previous reports of increased parietal atrophy in EOAD (1) were supported in our amnestic EOAD sample, given the significant interaction between age and diagnosis for parietal regions, indicating more prominent atrophy in the EOAD group than in LOAD. Additionally, we did observe higher levels of tau-PET uptake in parietal regions in the EOAD group, which may potentially contribute to the more pronounced atrophy in this region.

In comparison to respective controls, the amnestic AD groups show similar significant increased frequency or severity in the investigated co-pathologies. The only exception was

observed for WMH which were increased in EOAD, but not in LOAD, where the results were more inconsistent. The fact that the EOAD group shows a similar level of co-pathologies as LOAD may be due to faster accumulation of pathologies, such as tau, but could also reflect a lack of resilience to pathologies. The mechanisms behind the presence of these co-pathologies for EOAD despite younger age remains to be elucidated.

It is of interest that no differences between EOAD and LOAD were found for a common co-pathology, the proxy of TDP-43 pathology. Previously, it has been reported significantly less TDP-43 proteinopathy in EOAD compared to LOAD (5). This was not replicated in the present study using a proxy of TDP-43 based on the observed anterior to posterior gradient of TDP-43 occurrences in the MTL (41). It is possible that the proxy, established in an autopsy cohort, does not replicate to our cohort, even though a similar cut-off was found when replicating it in our cohort (693 vs. 645) using Gaussian mixture modeling without postmortem validation. The fact that no difference between AD groups was observed could, however, also be due to a smaller sample size compared to what the study by Spina and colleagues (5) included and the indirect nature of our measure for presence of TDP-43. Nevertheless, we did find that our measure of TDP-43 positivity was associated with lower hippocampal volume in the amnestic EOAD group. Lastly, previous studies have reported a higher burden of AD pathology in amnestic EOAD compared to LOAD (2,5,54). We found that amnestic EOAD shows more neocortical tau pathology while presenting similar levels of MTL tau to LOAD. Our results are, thus, in line with the notion of EOAD showing a more aggressive disease progression with faster cognitive decline and accumulation of pathology (1) and previous observations of higher levels of tau accumulation in younger individuals (55). The null results regarding our analyses associating co-pathologies with MTL structural measures in EOAD are likely due to limited power.

Strengths and Limitations

Strengths of the current study include the fine-grained investigation of MTL subfields, the use of a highly characterized cohort with various biomarkers of (co-)pathologies available, and the focus on amnestic EOAD as a separate group. Additionally, a new reliable automated segmentation for the whole amygdala is presented. However, the study also presents some limitations. First, the sample size of the EOAD group is relatively small. While this corresponds to the lower proportion of EOAD in the general population (56), it results in lower statistical power. Thus, future studies should investigate a larger sample of amnestic EOAD. Second, the cross-sectional nature of the study does not allow us to draw conclusions about potential more aggressive courses or larger atrophy rates between groups.

Conclusions

In summary, we found a largely similar MTL atrophy pattern in amnestic EOAD compared to LOAD. Interestingly, besides lower white matter hyperintensity volumes and higher neocortical tau PET in EOAD compared to LOAD, no differences in other AD- and co-pathologies, such as MTL tau-PET, and our proxy of TDP-43 were observed between EOAD and LOAD. These results suggests that the driving mechanisms of the amnestic symptoms in both groups might be largely similar and resulting in similar atrophy patterns within the MTL.

Data availability

Pseudo-anonymized data from BioFINDER-2 will be shared on request from a qualified academic investigator for the sole purpose of replicating procedures and results presented in the article and as long as data transfer is in agreement with EU legislation on the general data protection regulation and decisions by the Swedish Ethical Review Authority and Region Skåne, which should be regulated in a material transfer agreement.

Abbreviations

$\text{A}\beta$ = Amyloid-beta; AD = Alzheimer's disease; aHC = anterior Hippocampus; AMY = Amygdala; ANCOVA = Analysis of covariance; ASHS = Automated Segmentation of Hippocampal Subfields; BA35 = Brodmann area 35 (\approx transentorhinal cortex); CA1 = cornu ammonis 1; C.I. = confidence interval; CSF = cerebrospinal fluid; EOAD = early-onset Alzheimer's Disease; ERC = entorhinal cortex; LOAD = larly-onset Alzheimer's Disease; MTL = medial temporal lobe; NFTs = tau neurofibrillary tangles; PET = positron emission tomography; pHC = posterior Hippocampus; PHC = parahippocampal cortex; TDP-43 = transactive response DNA binding protein 43; WMH = white matter hyperintensities.

References

1. Mendez MF. Early-onset Alzheimer Disease and Its Variants. *Contin Minneap Minn.* 2019 Feb;25(1):34–51.
2. Marshall GA, Fairbanks LA, Tekin S, Vinters HV, Cummings JL. Early-Onset Alzheimer's Disease Is Associated With Greater Pathologic Burden. *J Geriatr Psychiatry Neurol.* 2007 Mar 1;20(1):29–33.
3. Aziz AL, Giusiano B, Joubert S, Duprat L, Didic M, Gueriot C, et al. Difference in imaging biomarkers of neurodegeneration between early and late-onset amnestic Alzheimer's disease. *Neurobiol Aging.* 2017 Jun 1;54:22–30.
4. Polsinelli AJ, Logan PE, Lane KA, Manchella MK, Nemes S, Sanjay AB, et al. APOE ϵ 4 carrier status and sex differentiate rates of cognitive decline in early- and late-onset Alzheimer's disease. *Alzheimers Dement [Internet].* 2023 [cited 2023 Apr 24];n/a(n/a). Available from: <https://doi.org/10.1002/alz.12831>

5. Spina S, La Joie R, Petersen C, Nolan AL, Cuevas D, Cosme C, et al. Comorbid neuropathological diagnoses in early versus late-onset Alzheimer's disease. *Brain J Neurol.* 2021 Aug 17;144(7):2186–98.
6. Tanner JA, Iaccarino L, Edwards L, Asken BM, Gorno-Tempini ML, Kramer JH, et al. Amyloid, tau and metabolic PET correlates of cognition in early and late-onset Alzheimer's disease. *Brain.* 2022 Jun 28;awac229.
7. Hammers DB, Eloyan A, Taurone A, Thangarajah M, Beckett L, Gao S, et al. Profiling baseline performance on the Longitudinal Early-Onset Alzheimer's Disease Study (LEADS) cohort near the midpoint of data collection. *Alzheimers Dement [Internet].* 2023 May 31 [cited 2023 Sep 5];n/a(n/a). Available from: <https://doi.org/10.1002/alz.13160>
8. Cho H, Jeon S, Kang SJ, Lee JM, Lee JH, Kim GH, et al. Longitudinal changes of cortical thickness in early- versus late-onset Alzheimer's disease. *Neurobiol Aging.* 2013 Jul 1;34(7):1921.e9-1921.e15.
9. Hamelin L, Bertoux M, Bottlaender M, Corne H, Lagarde J, Hahn V, et al. Sulcal morphology as a new imaging marker for the diagnosis of early onset Alzheimer's disease. *Neurobiol Aging.* 2015 Nov;36(11):2932–9.
10. Migliaccio R, Agosta F, Possin KL, Canu E, Filippi M, Rabinovici GD, et al. Mapping the Progression of Atrophy in Early- and Late-Onset Alzheimer's Disease. *J Alzheimers Dis JAD.* 2015;46(2):351–64.
11. Squire LR, Zola-Morgan S. The medial temporal lobe memory system. *Science.* 1991 Sep 20;253(5026):1380–6.

12. Eichenbaum H, Otto T, Cohen NJ. Two functional components of the hippocampal memory system. *Behav Brain Sci.* 1994 Sep;17(3):449–72.
13. Ritchey M, Libby LA, Ranganath C. Cortico-hippocampal systems involved in memory and cognition: the PMAT framework. *Prog Brain Res.* 2015;219:45–64.
14. Braak H, Braak E. Neuropathological staging of Alzheimer-related changes. *Acta Neuropathol (Berl).* 1991 Sep 1;82(4):239–59.
15. Llamas-Rodríguez J, Oltmer J, Greve DN, Williams E, Slepneva N, Wang R, et al. Entorhinal Subfield Vulnerability to Neurofibrillary Tangles in Aging and the Preclinical Stage of Alzheimer’s Disease. *J Alzheimers Dis.* 2022;87(3):1379–99.
16. Wisse LEM, Ravikumar S, Ittyerah R, Lim S, Lane J, Bedard ML, et al. Downstream effects of polypathology on neurodegeneration of medial temporal lobe subregions. *Acta Neuropathol Commun.* 2021 Jul 21;9(1):128.
17. Knopman DS, Amieva H, Petersen RC, Chételat G, Holtzman DM, Hyman BT, et al. Alzheimer disease. *Nat Rev Dis Primer.* 2021 May 13;7(1):33.
18. Rabinovici GD, Carrillo MC, Forman M, DeSanti S, Miller DS, Kozauer N, et al. Multiple comorbid neuropathologies in the setting of Alzheimer’s disease neuropathology and implications for drug development. *Alzheimers Dement Transl Res Clin Interv.* 2017 Jan 1;3(1):83–91.
19. Palmqvist S, Rossi M, Hall S, Quadalti C, Mattsson-Carlgren N, Dellavalle S, et al. Cognitive effects of Lewy body pathology in clinically unimpaired individuals. *Nat Med.* 2023 Aug 1;29(8):1971–8.

20. Tosun D, Yardibi O, Benzinger TLS, Kukull WA, Masters CL, Perrin RJ, et al. Identifying individuals with non-Alzheimer's disease co-pathologies: A precision medicine approach to clinical trials in sporadic Alzheimer's disease. *Alzheimers Dement [Internet]*. 2023 Sep 4 [cited 2023 Nov 1];n/a(n/a). Available from: <https://doi.org/10.1002/alz.13447>

21. Kapasi A, DeCarli C, Schneider JA. Impact of multiple pathologies on the threshold for clinically overt dementia. *Acta Neuropathol (Berl)*. 2017 Aug 1;134(2):171–86.

22. Nelson PT, Dickson DW, Trojanowski JQ, Jack CR, Boyle PA, Arfanakis K, et al. Limbic-predominant age-related TDP-43 encephalopathy (LATE): consensus working group report. *Brain*. 2019 Jun 1;142(6):1503–27.

23. Palmqvist S, Janelidze S, Quiroz YT, Zetterberg H, Lopera F, Stomrud E, et al. Discriminative Accuracy of Plasma Phospho-tau217 for Alzheimer Disease vs Other Neurodegenerative Disorders. *JAMA*. 2020 Aug 25;324(8):772–81.

24. Connor DJ, Sabbagh MN. Administration and Scoring Variance on the ADAS-Cog. *J Alzheimers Dis*. 2008;15(3):461–4.

25. Hansson O, Seibyl J, Stomrud E, Zetterberg H, Trojanowski JQ, Bittner T, et al. CSF biomarkers of Alzheimer's disease concord with amyloid- β PET and predict clinical progression: A study of fully automated immunoassays in BioFINDER and ADNI cohorts. *Alzheimers Dement*. 2018 Nov 1;14(11):1470–81.

26. Hansson O, Batrla R, Brix B, Carrillo MC, Corradini V, Edelmayer RM, et al. The Alzheimer's Association international guidelines for handling of cerebrospinal fluid for routine clinical measurements of amyloid β and tau. *Alzheimers Dement*. 2021 Sep 1;17(9):1575–82.

27. Janelidze S, Stomrud E, Brix B, Hansson O. Towards a unified protocol for handling of CSF before β -amyloid measurements. *Alzheimers Res Ther*. 2019 Jul 19;11(1):63.
28. Gobom J, Parnetti L, Rosa-Neto P, Vyhalek M, Gauthier S, Cataldi S, et al. Validation of the LUMIPULSE automated immunoassay for the measurement of core AD biomarkers in cerebrospinal fluid. 2022;60(2):207–19.
29. Palmqvist S, Janelidze S, Quiroz YT, Zetterberg H, Lopera F, Stomrud E, et al. Discriminative Accuracy of Plasma Phospho-tau217 for Alzheimer Disease vs Other Neurodegenerative Disorders. *JAMA*. 2020 Aug 25;324(8):772–81.
30. Pichet Binette A, Franzmeier N, Spotorno N, Ewers M, Brendel M, Biel D, et al. Amyloid-associated increases in soluble tau relate to tau aggregation rates and cognitive decline in early Alzheimer's disease. *Nat Commun*. 2022 Nov 4;13(1):6635.
31. Folstein MF, Folstein SE, McHugh PR. “Mini-mental state”: A practical method for grading the cognitive state of patients for the clinician. *J Psychiatr Res*. 1975 Nov 1;12(3):189–98.
32. Lezak MD. Neuropsychological assessment. [Internet]. 5. ed. Oxford University Press; 2012. Available from: <http://ludwig.lub.lu.se/login?url=https://search.ebscohost.com/login.aspx?direct=true&db=cat07147a&AN=lub.4785165&site=eds-live&scope=site>
33. Mack WJ, Freed DM, Williams BW, Henderson VW. Boston Naming Test: Shortened Versions for Use in Alzheimer's Disease. *J Gerontol*. 1992 May 1;47(3):P154–8.
34. Reitan RM. Validity of the Trail Making Test as an Indicator of Organic Brain Damage. *Percept Mot Skills*. 1958 Dec 1;8(3):271–6.

35. Smith A. Symbol digit modalities test. Western psychological services Los Angeles; 1973.
36. Warrington EK, James M, Thames Valley Test Company. The visual object and space perception battery. Bury St. Edmunds: Thames Valley Test Company Bury St. Edmunds; 1991.
37. Berron D, Vieweg P, Hochkeppler A, Pluta JB, Ding SL, Maass A, et al. A protocol for manual segmentation of medial temporal lobe subregions in 7Tesla MRI. *NeuroImage Clin.* 2017 Jan 1;15:466–82.
38. Xie L, Wisse LEM, Pluta J, de Flores R, Piskin V, Manjón JV, et al. Automated segmentation of medial temporal lobe subregions on in vivo T1-weighted MRI in early stages of Alzheimer’s disease. *Hum Brain Mapp.* 2019 Aug 15;40(12):3431–51.
39. Xie L, Wisse LEM, Wang J, Ravikumar S, Khandelwal P, Glenn T, et al. Deep label fusion: A generalizable hybrid multi-atlas and deep convolutional neural network for medical image segmentation. *Med Image Anal.* 2023 Jan 1;83:102683.
40. Yushkevich PA, Pluta JB, Wang H, Xie L, Ding SL, Gertje EC, et al. Automated volumetry and regional thickness analysis of hippocampal subfields and medial temporal cortical structures in mild cognitive impairment. *Hum Brain Mapp.* 2015 Jan 1;36(1):258–87.
41. de Flores R, Wisse LEM, Das SR, Xie L, McMillan CT, Trojanowski JQ, et al. Contribution of mixed pathology to medial temporal lobe atrophy in Alzheimer’s disease. *Alzheimers Dement.* 2020 Jun 1;16(6):843–52.

42. Touroutoglou A, Katsumi Y, Brickhouse M, Zaitsev A, Eckbo R, Aisen P, et al. The Sporadic Early-onset Alzheimer's Disease Signature Of Atrophy: Preliminary Findings From The Longitudinal Early-onset Alzheimer's Disease Study (LEADS) Cohort. *Alzheimers Dement [Internet]*. 2023 Oct 18 [cited 2023 Nov 8];n/a(n/a). Available from: <https://doi.org/10.1002/alz.13466>

43. Leuzy A, Smith R, Ossenkoppele R, Santillo A, Borroni E, Klein G, et al. Diagnostic Performance of RO948 F 18 Tau Positron Emission Tomography in the Differentiation of Alzheimer Disease From Other Neurodegenerative Disorders. *JAMA Neurol*. 2020 Aug 1;77(8):955–65.

44. Baker SL, Maass A, Jagust WJ. Considerations and code for partial volume correcting [18F]-AV-1451 tau PET data. *Data Brief*. 2017 Dec 1;15:648–57.

45. Rousset OG, Ma Y, Evans AC. Correction for partial volume effects in PET: principle and validation. *J Nucl Med*. 1998;39(5):904–11.

46. Cho H, Choi J, Hwang M, Kim Y, Lee H, Lee H, et al. In Vivo Cortical Spreading Pattern of Tau and Amyloid in the Alzheimer Disease Spectrum. *Ann Neurol*. 2016 Aug;80(2):247–58.

47. Leuzy A, Smith R, Cullen NC, Strandberg O, Vogel JW, Binette AP, et al. Biomarker-Based Prediction of Longitudinal Tau Positron Emission Tomography in Alzheimer Disease. *JAMA Neurol*. 2022 Feb 1;79(2):149–58.

48. Cerri S, Puonti O, Meier DS, Wuerfel J, Mühlau M, Siebner HR, et al. A contrast-adaptive method for simultaneous whole-brain and lesion segmentation in multiple sclerosis. *NeuroImage*. 2021 Jan;225:117471.

49. Puonti O, Iglesias JE, Van Leemput K. Fast and sequence-adaptive whole-brain segmentation using parametric Bayesian modeling. *NeuroImage*. 2016 Dec;143:235–49.

50. R Core Team. R: A language and environment for statistical computing. Vienna, Austria: R Foundation for Statistical Computing; 2020.

51. Chishiki Y, Hirano S, Li H, Kojima K, Nakano Y, Sakurai T, et al. Different Patterns of Gray Matter Volume Reduction in Early-onset and Late-onset Alzheimer Disease. *Cogn Behav Neurol Off J Soc Behav Cogn Neurol*. 2020 Dec;33(4):253–8.

52. Lee EC, Kang JM, Seo S, Seo HE, Lee SY, Park KH, et al. Association of Subcortical Structural Shapes With Tau, Amyloid, and Cortical Atrophy in Early-Onset and Late-Onset Alzheimer’s Disease. *Front Aging Neurosci*. 2020;12:563559.

53. Ossenkoppele R, Mattsson N, Teunissen CE, Barkhof F, Pijnenburg Y, Scheltens P, et al. Cerebrospinal Fluid Biomarkers and Cerebral Atrophy in Distinct Clinical Variants of Probable Alzheimer’s Disease. *Neurobiol Aging*. 2015 Aug;36(8):2340–7.

54. Visser D, Verfaillie SCJ, Wolters EE, Coomans EM, Timmers T, Tuncel H, et al. Differential associations between neocortical tau pathology and blood flow with cognitive deficits in early-onset vs late-onset Alzheimer’s disease. *Eur J Nucl Med Mol Imaging*. 2022 May 1;49(6):1951–63.

55. Smith R, Strandberg O, Mattsson-Carlsgren N, Leuzy A, Palmqvist S, Pontecorvo MJ, et al. The accumulation rate of tau aggregates is higher in females and younger amyloid-positive subjects. *Brain*. 2020 Dec 1;143(12):3805–15.

56. Zhu XC, Tan L, Wang HF, Jiang T, Cao L, Wang C, et al. Rate of early onset Alzheimer’s disease: a systematic review and meta-analysis. *Ann Transl Med* Vol 3 No 3

March 10 2015 Ann Transl Med [Internet]. 2015 [cited 2015 Jan 1]; Available from: <https://atm.amegroups.org/article/view/5826>

Acknowledgements

We would like to acknowledge all the BioFINDER team members as well as participants in the study and their family members for their dedication. This study was supported by MultiPark - A Strategic Research Area at Lund University.

Funding

This study was supported by MultiPark - A Strategic Research Area at Lund University. Additionally, this work was supported by project grants from NIA (R01-AG070592, R01-AG069474, RF1-AG056014), the Swedish Research Council (2022-00900), Alzheimerfonden (AF980872, AF993465) and the Crafoord foundation (20210690).

The BioFINDER-2 study was supported by the European Research Council (ADG-101096455), Alzheimer's Association (ZEN24-1069572, SG-23-1061717), GHR Foundation, Swedish Research Council (2022-00775, 2018-02052, 2021-02219), ERA PerMed (ERAPERMED2021-184), the Knut and Alice Wallenberg foundation (2022-0231), the Strategic Research Area MultiPark (Multidisciplinary Research in Parkinson's disease) at Lund University, the Swedish Alzheimer Foundation (AF-980907, AF-980832, AF-994229), the Swedish Brain Foundation (FO2021-0293, FO2022-0204, FO2023-0163), The Parkinson foundation of Sweden (1412/22), Familjen Rönnströms Stiftelse (FRS-0003), WASP and DDLS Joint call for research projects (WASP/DDLS22-066), the Cure Alzheimer's fund, the Konung Gustaf V:s och Drottning Victorias Frimurarestiftelse, the Skåne University Hospital Foundation (2020-O000028), Regionalt Forskningsstöd (2022-1259) and the Swedish federal government under the ALF agreement (2022-Projekt0280, 2022-Projekt0107). The

precursor of ¹⁸F-flutemetamol was sponsored by GE Healthcare. A.P.B. is supported by a postdoctoral fellowship from the Fonds de recherche en Santé Québec (298314).

The funding sources had no role in the design and conduct of the study; in the collection, analysis, interpretation of the data; or in the preparation, review, or approval of the manuscript.

Author information

Nicola Spotorno and Laura E.M. Wisse share co-last/equal authorship.

Corresponding authors

Correspondence to Laura E.M. Wisse or Anika Wuestefeld.

Ethics declaration

Ethics approval and consent to participate

The study was approved by the Regionala Etiksprövningsnämnden i Lund (regional ethical review board in Lund), Sweden, and all study participants provided written informed consent in accordance with the Declaration of Helsinki.

Competing interests

A.W., A.P.B., H.B., E.S., O.S., D.W., N.M.-C, N.S., P.A.Y., and L.E.M.W. have nothing to declare. D.B. is co-founder of neotiv GmbH. R.S. has received a speaker fee from Roche. S.P. has acquired research support (for the institution) from ki elements / ADDF and Avid. In the past 2 years, he has received consultancy/speaker fees from Bioartic, Biogen, Esai, Lilly, and Roche. O.H. has acquired research support (for the institution) from AVID Radiopharmaceuticals, Biogen, C2N Diagnostics, Eli Lilly, Eisai, Fujirebio, GE Healthcare, and Roche. In the past 2 years, he has received consultancy/speaker fees from AC Immune, Alzpath, BioArctic, Biogen, Bristol Meyer Squibb, Cerveau, Eisai, Eli Lilly, Fujirebio, Merck, Novartis, Novo Nordisk, Roche, Sanofi and Siemens.

Supplementary information

Supplementary material is available: supplementary methods and supplementary results.